STEM CELLS TRANSLATIONAL MEDICINE®

FETAL AND NEONATAL STEM CELLS

Conditioned Medium From Human Amniotic Mesenchymal Stromal Cells Limits Infarct Size and Enhances Angiogenesis

PATRIZIA DANIELI,[a,b,*] GIUSEPPE MALPASSO,[a,b,c,*] MARIA CHIARA CIUFFREDA,[a,b,*] ELISABETTA CERVIO,[a,b] LAURA CALVILLO,[d] FRANCESCO COPES,[a,b] FEDERICA PISANO,[a,b] MANUELA MURA,[a,b] LENNAERT KLEIJN,[e] RUDOLF A. DE BOER,[e] GIANLUCA VIARENGO,[f] VITTORIO ROSTI,[g] ARSENIO SPINILLO,[h] MARIANNA ROCCIO,[h] MASSIMILIANO GNECCHI[a,b,c,i]

[a]Department of Cardiothoracic and Vascular Sciences, Coronary Care Unit and Laboratory of Clinical and Experimental Cardiology, [b]Laboratory of Experimental Cardiology for Cell and Molecular Therapy, [f]Division of Clinical Immunology, Immunohematology, and Transfusion Service, [g]Center for the Study and Cure of Myelofibrosis, Biotechnology Research Laboratories, and [h]Division of Obstetrics and Gynecology, Fondazione IRCCS Policlinico San Matteo, Pavia, Italy; [c]Department of Molecular Medicine, Unit of Cardiology, University of Pavia, Pavia, Italy; [d]Laboratory of Cardiovascular Genetics, IRCCS Istituto Auxologico Italiano, Milan, Italy; [e]Department of Cardiology, University Medical Center Groningen, Groningen, The Netherlands; [i]Department of Medicine, University of Cape Town, Cape Town, South Africa

[*]Contributed equally.

Correspondence: Massimiliano Gnecchi, M.D., Ph.D., Department of Cardiothoracic and Vascular Sciences, Coronary Care Unit and Laboratory of Clinical and Experimental Cardiology, Fondazione IRCCS Policlinico San Matteo, Viale Golgi, 19, 27100 Pavia, Italy. Telephone: 39-0382-501-881. E-Mail: m.gnecchi@unipv.it

Received November 5, 2014; accepted for publication February 2, 2015; published Online First on March 30, 2015.

1066-5099/2015/$20.00/0

http://dx.doi.org/10.5966/sctm.2014-0253

Key Words. Cardiac • Fetal stem cells • Clinical translation • Placenta

ABSTRACT

The paracrine properties of human amniotic membrane-derived mesenchymal stromal cells (hAMCs) have not been fully elucidated. The goal of the present study was to elucidate whether hAMCs can exert beneficial paracrine effects on infarcted rat hearts, in particular through cardioprotection and angiogenesis. Moreover, we aimed to identify the putative active paracrine mediators. hAMCs were isolated, expanded, and characterized. In vitro, conditioned medium from hAMC (hAMC-CM) exhibited cytoprotective and proangiogenic properties. In vivo, injection of hAMC-CM into infarcted rat hearts limited the infarct size, reduced cardiomyocyte apoptosis and ventricular remodeling, and strongly promoted capillary formation at the infarct border zone. Gene array analysis led to the identification of 32 genes encoding for the secreted factors overexpressed by hAMCs. Among these, midkine and secreted protein acidic and rich in cysteine were also upregulated at the protein level. Furthermore, high amounts of several proangiogenic factors were detected in hAMC-CM by cytokine array. Our results strongly support the concept that the administration of hAMC-CM favors the repair process after acute myocardial infarction. STEM CELLS TRANSLATIONAL MEDICINE *2015;4:448–458*

SIGNIFICANCE

The demonstration that stem cells repair infarcted hearts mainly through paracrine mechanisms represents a potential breakthrough. Characterization of therapeutic paracrine mediators could lead to the possibility of treating acute myocardial infarction (AMI) with a single stem cell-derived molecule or a mixture. Compared with cell therapy, this approach would be technically easier to translate to the bedside. An even more straightforward strategy consists of the administration of the entire stem cell secretome (i.e., conditioned medium [CM]). Despite these potential advantages, this approach has not been thoroughly investigated using human cells. This study shows that CM of fetal stromal cells (human amniotic membrane-derived mesenchymal stromal cell [hAMC]-CM), derived from an ethically acceptable source such as the placenta, can repair infarcted hearts without the need for any manipulation. The use of hAMC-CM might be readily translated to the clinical arena in the setting of AMI upon demonstration of its effectiveness in a large animal model.

INTRODUCTION

Adult stem cell therapy is a promising approach to repair postischemic myocardial damage [1]. In particular, transplantation of adult bone marrow-derived mesenchymal stromal cells (BM-MSCs) has provided encouraging results in animal models of myocardial infarction, in terms of both prevention of left ventricular (LV) remodeling and recovery of cardiac function; however, the mechanisms of action are still unclear [2]. Differentiation of BM-MSCs into cardiomyocytes (CMCs) occurs at a very low frequency [3], and it has been convincingly proved that MSCs, through the secretion of soluble paracrine factors [4], protect the heart [5, 6], promote neovascularization [7], preserve cardiac metabolism [8], and mediate endogenous regeneration via activation of resident cardiac progenitor cells [9].

The demonstration of stem cell paracrine mechanisms in myocardial repair represents a step forward in the translation of cell-based therapies to the clinical arena, because it might be possible to

use soluble factors rather than MSCs to treat ischemic damage. This is particularly true in the acute setting, in which cardiac protection, rather than tissue regeneration, could be considered a reasonable therapeutic goal.

Recently, it has been reported that multipotent MSCs of fetal origin can be isolated from the amniotic membrane of human placenta (hAMCs) [10]. These cells display a wide phenotypic and cellular plasticity [11, 12], are immunologically tolerated [13], and are apparently able to differentiate into mature and competent CMCs in vitro and regenerate cardiac tissue in vivo. However, the paracrine properties of hAMCs have never been investigated in depth. Therefore, we aimed to verify whether hAMCs can exert beneficial paracrine effects. In particular, we tested the effects of conditioned medium (CM) obtained from hAMCs (hAMC-CM) on cardiac protection and neovascularization both in vitro and in vivo. Moreover, we searched for putative active soluble factors mediating the paracrine effects exerted by the hAMCs.

Materials and Methods

Isolation and Culture of hAMCs

Human term placentas were donated by healthy mothers undergoing cesarean section. The Ethical Committee of the Fondazione IRCCS Policlinico San Matteo approved the study, which was performed in accordance with the Declaration of Helsinki. All samples were collected after obtaining informed consent from the donors. Fragments of the amniotic membrane were digested in 0.25% trypsin-EDTA for 2 hours and subsequently in 50 U/ml collagenase for 2 hours (Sigma-Aldrich, St. Louis, MO, http://www.sigmaaldrich.com) in Hanks' balanced salt solution (Celbio, EuroClone Group, Milan, Italy, http://www.euroclone.it). The supernatant was collected and centrifuged at 200*g* for 10 minutes. Harvested cells were cultured in polystyrene culture dishes (Corning Inc., Corning, NY, http://www.corning.com) at 37°C with an atmosphere of 5% CO_2 and 95% N_2 and in α-minimum essential medium (Celbio EuroClone Group) supplemented with 10% fetal bovine serum, 2 mmol/l L-glutamine, 100 U/ml penicillin, and 100 μg/ml streptomycin (all from Gibco, Life Technologies, Carlsbad, CA, http://www.lifetechnologies.com). hAMCs were selected by plastic adherence and propagated in culture.

Generation of Conditioned Medium

hAMC-CM and human dermal fibroblast CM (fib-CM) were generated as follows: 90% confluent cells were fed with serum-free Dulbecco's modified Eagle medium (DMEM) high glucose and incubated for 36 hours at 37°C. Control medium (CTRL-M) was obtained under the same conditions in the absence of cells. Cell debris was precipitated by centrifugation at 4°C at 4,000*g*, and CM was transferred to a new tube stored at −80°C until needed. For the in vitro experiments, we used a 1:1 ratio of target cells/hAMCs or fibroblasts. For example, for 1,000 target cells, we used CM produced by 1,000 cells (hAMCs or fibroblasts).

Concentrated CM for animal experiments was generated as follows: hAMC or fibroblasts were fed with serum-free DMEM high glucose and cultured for 36 hours. The medium was then collected, and the cells were counted for normalization purposes. For each animal, we used medium generated by 2×10^6 cells. After removing cell debris as described, the supernatant was transferred to dedicated ultrafiltration tubes with 3,000 nominal molecular weight limit (Amicon Ultra-3K device; EMD Millipore, Bedford, MA, http://www.emdmillipore.com), concentrated by centrifugation at 4,000*g* for 1 hour at 4°C and desalted according to the manufacturer's protocol. The final volume was 150 μl per single dose. CM was frozen at −80°C and used in subsequent experiments.

H9c2 Cell Culture and Hypoxia/Reoxygenation Protocol

The H9c2 embryonic rat heart-derived cell line was obtained from the American Type Culture Collection (CRL-1446) and cultured according to the manufacturer's protocol. Before each experiment, H9c2 cells were serum starved for 24 hours to stop cell proliferation. To induce hypoxia/reoxygenation (H/R) injury, H9c2 cells were incubated under hypoxic conditions for 6 hours inside an airtight Plexiglas chamber with an atmosphere of 5% CO_2 and 95% N_2 at 37°C. The oxygen level in the chamber was $<0.5\%$ (oxygen analyzer $MAXO_2$; Maxtec, Salt Lake City, UT, http://www.maxtec.com). H9c2 cells were then reoxygenated in a normoxic environment at 37°C for 18 hours in the presence of CTRL-M, hAMC-CM, or fib-CM.

Viability and Apoptosis Assays

CellTiter96 Aqueous One Solution Cell viability assay (MTS) (Promega, Madison, WI, http://www.promega.com) was used according to the manufacturer's instructions. terminal deoxynucleotidyl transferase dUTP nick-end labeling (TUNEL) was performed using DeadEnd Fluorometric TUNEL System Assays (Promega) according to a standard protocol. Nuclei were stained with Hoechst 33258 (Sigma-Aldrich). The samples were mounted with Vectashield mounting medium (Vector Laboratories Inc., Burlingame, CA, http://www.vectorlabs.com) and examined using a Zeiss Axio Observer Z1 Apotome microscope (Carl Zeiss, Milan, Italy, http://www.zeiss.com). Caspase-3 activation was measured by Western blot and the colorimetric activity assay kit (Sigma-Aldrich), according to the manufacturer's instructions.

Endothelial Progenitor Cell Migration and Matrigel Assay

The migration assay was performed using a modified Boyden chamber (Transwell; Corning Inc.) assay. In brief, endothelial progenitor cells (EPCs) were seeded on a polycarbonate membrane (8-μm pores) in 24-well Transwell plates in the presence of endothelial growth medium 2 (EGM2) alone or supplemented with 10 ng/ml stromal cell derived factor-1α (SDF-1α; positive control), CTRL-M (negative control), or hAMC-CM or fib-CM at different concentrations (1×, 10×, and 50×). After 10 hours, EPCs that had migrated to the lower side of the membrane were counted in 5 random microscopic fields. For the angiogenesis assay, EPCs were seeded in 15 mg/ml Matrigel (Cultrex BME; Trevigen, Gaithersburg, MD, http://www.trevigen.com) in the presence of hAMC-CM or fib-CM at different concentrations (1×, 10×, 20×). CTRL-M and EGM2 were used as negative and positive controls, respectively. Tube formation was assessed after 5, 24, 48, and 72 hours. The images were captured with a camera connected to a phase-contrast microscope. We performed three independent experiments, and the number of branch points was manually counted.

Surgical Procedures and Animal Study Design

Before surgery, the rats were randomized to 3 groups. The control rats received a saline injection, and the CM-treated rats

received either hAMC-CM or fib-CM. We used male Sprague-Dawley rats, weighing 175–200 g (Charles River Research Models and Services, Calco, Italy, http://www.criver.com). The rats were anesthetized by administering 5% isoflurane during oxygen delivery inside an induction chamber and pretreated with ampicillin (100 mg/kg) and carprofen (5 mg/kg). The rats were intubated endotracheally, artificially ventilated with a rodent ventilator, and electrocardiographically monitored throughout the surgical procedures. The chest was opened, and the heart was exteriorized through the intercostal space. To induce ischemic injury, the left anterior descending coronary artery (LAD) was ligated for 30 minutes. Ischemia was confirmed by bleaching of the anterior wall of the left ventricle (LV) and ST elevation on the electrocardiogram (ECG). After occlusion, the LAD ligature was released, and reperfusion was confirmed by the restoration of a bright red tissue color and the presence of arrhythmias monitored by the ECG trace. After 10 minutes, a total of 150 μl of saline, hAMC-CM, or fib-CM was injected into 5 different sites of the infarct border zone. After 48 hours, 10 rats per group were sacrificed for quantification of the infarct size and apoptotic index. The remaining rats (n = 10 per each group) were sacrificed after 30 days for capillary density quantification and morphometric analysis. The investigators responsible for surgery and injections were unaware of the treatment groups. All procedures for the care and treatment of the rats were performed according to the approved protocols and animal welfare regulations of the University of Pavia Ethical Committee and the Animal Care Committee of the Italian Ministry of Health (in accordance with Italian DL-116/92 and the Directive 2010/63/EU of the European Parliament and the Council).

Infarct Size Quantification

After 48 hours, the rats were sacrificed to determine the infarct size. The rats were anesthetized and ventilated, and the thorax was surgically opened. We performed a small excision at the level of the right atrium and then started heart perfusion with phosphate-buffered saline containing heparin. When the heart was bleached, the LAD was reoccluded using the silk suture left in place after the first surgery, the pulmonary artery and aorta were clamped, and 2×10^6 fluorescent microspheres, 10 μm in diameter (540/560 nm; Molecular Probes; Life Technologies) were injected into the LV cavity. After 15 seconds, the clamps were removed, and the heart was immediately arrested by injecting 0.2 N KCl, removed from the chest, and manually sectioned transversally from the apex to the base into five 2-mm-thick biventricular sections.

To quantify the area at risk (AAR) and the infarct size (IS), the heart sections were incubated in a 1% 2,3,5-triphenyltetrazolium chloride solution (Sigma-Aldrich) at 37°C for 5 minutes and fixed in 10% phosphate-buffered formalin. Both sides of each section were photographed under fluorescent and white light using a digital camera connected to a fluorescent stereomicroscope (Axio Zoom V16; Carl Zeiss). The total LV area, the infarct scar area, and the perfused zone were traced manually and measured using the software ImageJ (NIH, Bethesda, MD, USA, http://www.imagej.nih.gov/ij/, 1997–2012). The AAR, identified as the zone not reached by the fluorescent microspheres, was obtained by subtracting the perfused area from the total LV area. The IS, expressed as a percentage, was calculated by dividing the infarct area of each section by the corresponding AAR and multiplying by 100. For each heart, the mean of the IS/AAR was calculated. The investigators conducting the experiment were unaware of the experimental groups.

Detailed methods describing the TUNEL and immunohistochemical analyses are reported in the supplemental online data.

Gene Array

Total RNA was isolated from cultured hAMCs (n = 8), and fibroblasts (n = 6) after 48 hours of serum starvation. RNA was extracted with the Trizol reagent (Life Technologies) following the manufacturer's instructions. RNA amplification and labeling was performed with the Illumina TotalPrep 96 RNA Amplification Kit (Applied Biosystems, http://www.appliedbiosystems.com). Human HT-12 V3 Expression Bead Chip arrays (Illumina, San Diego, CA, http://www.illumina.com), targeting 37,812 annotated genes with 48,813 different probes designed using the RefSeq (Build 36.2, Release 22) and the UniGene (Build 199) databases (National Center for Biotechnology Information, Bethesda, MD, http://www.ncbi.nlm.nih.gov) were processed according to the manufacturer's protocol. The slides were scanned using an Illumina BeadArray Reader, and data were analyzed with Genome Studio and Genespring GX software (Agilent Technologies Santa Clara, CA, http://www.agilent.com).

The data discussed in the present report have been deposited in NCBI's Gene Expression Omnibus [14] and are accessible through GEO Series accession number GSE61153 (available at http://www.ncbi.nlm.nih.gov/geo/query/acc.cgi?acc=GSE61153).

Gene array data were validated by quantitative reverse transcription polymerase chain reaction (PCR) using SYBR green (Applied Biosystems) on a 7900HT Fast Real-Time PCR System (Applied Biosystems) according to standard procedures.

Statistical Analysis

All results are presented as the mean $\pm$ SD. Statistical analysis was performed with the standard parametric test one-way analysis of variance (ANOVA) using the Bonferroni method. The nonparametric ANOVA Kruskal-Wallis test was used in the case of nonhomogeneous variances. For cytokine array analysis, statistical significance was determined using the unpaired t test. The Mann-Whitney U test was applied after evaluation of nonhomogeneous variances. All statistical calculations were made using InStat software (GraphPad Software, Inc., San Diego, CA, http://www.graphpad.com).

Gene array data were analyzed using the Genome Studio and Genespring GX software (Agilent Technologies). The genes with significantly different levels of expression were chosen based on a log-twofold change >2 in gene expression, t test $p < .05$, and corrected for multiple testing using the Benjamini-Hochberg method.

All other methods are described in the supplemental online data.

Results

The hAMCs isolated in our laboratory displayed the phenotype typical of MSC. They stained positive for CD90, CD105, CD73, human leukocyte antigen (HLA)-ABC and negative for CD45, CD34, CD14, CD31, CD133, HLA-DR, and CD80. They also efficiently differentiated into both osteocytes and adipocytes in vitro (Fig. 1).

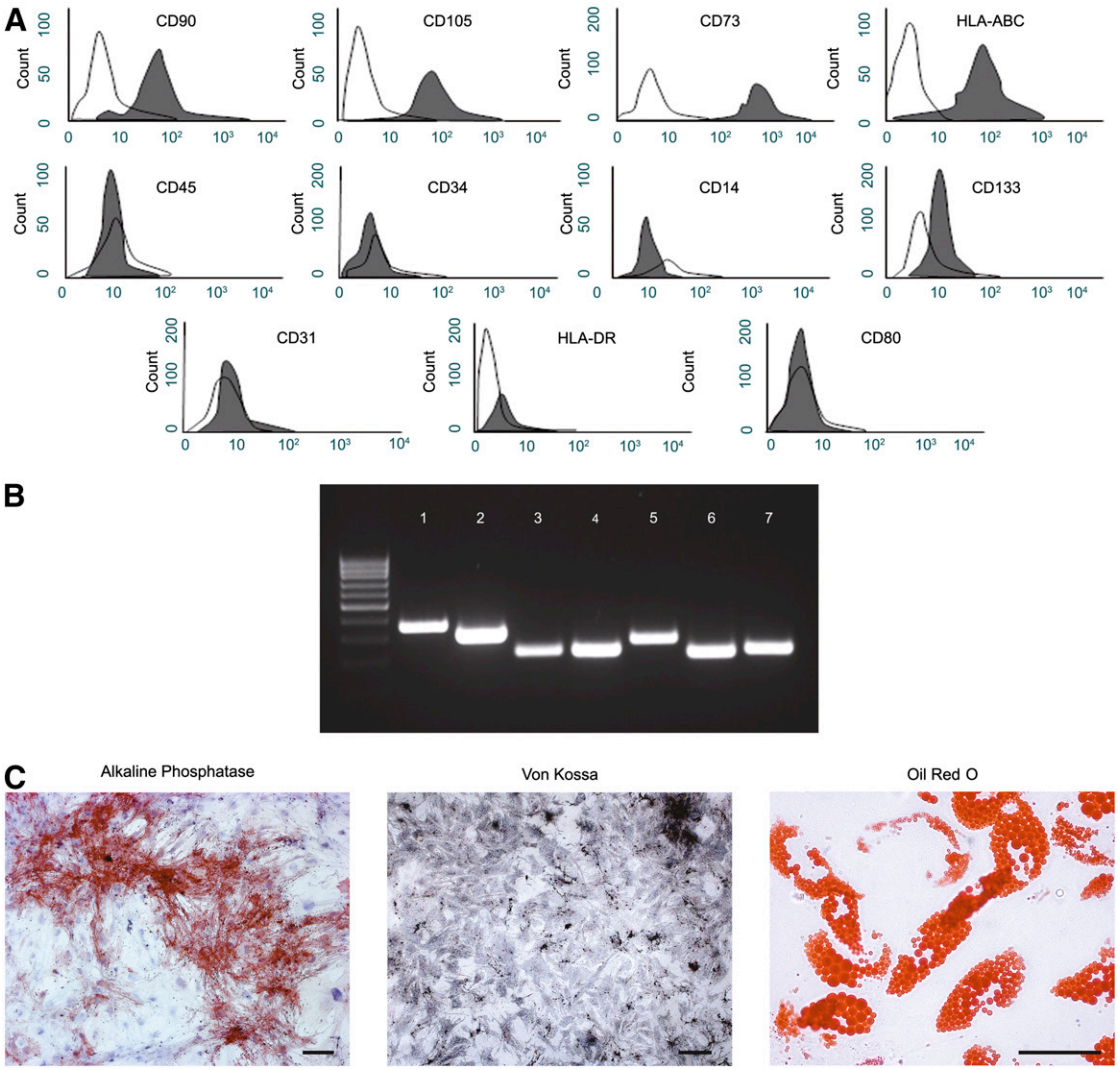

Figure 1. Characterization of human amniotic membrane-derived mesenchymal stromal cells (hAMCs). **(A):** Fluorescence-activated cell sorting analysis of hAMCs at passage 3. **(B):** Reverse transcription-polymerase chain reaction analysis for osteocyte markers osteopontin (band 1), cathepsin K (band 2), and bone sialoprotein (band 3) or adipocyte markers peroxisome proliferation-activated receptor γ (band 5) and adipose differentiation-related protein (band 6), after an osteogenic or adipogenic differentiation assay. Glyceraldehyde 6-phosphate dehydrogenase (bands 4 and 7) was used as an endogenous control. **(C):** Cytochemical analysis: alkaline phosphatase activity assay (bright field, scale bar = 100 μm) and Von Kossa staining (bright field, scale bar = 100 μm) of hAMCs after osteogenic induction and Oil Red O staining (bright field, scale bar = 50 μm) of hAMCs at the end of the adipogenic differentiation assay. Data are representative of three independent experiments. Abbreviation: HLA, human leukocyte antigen.

The results of several in vitro assays demonstrated that the factors secreted by hAMCs are cytoprotective and proangiogenic. First we showed that hAMC-CM prevents cell death. When rat H9c2 cardiomyoblasts were exposed to H/R in the presence of hAMC-CM, a significant increase in cell viability was observed compared with those in CTRL-M (+2.6-fold; $p <$ .001) or fib-CM (+1.7-fold; $p <$ .001) (Fig. 2A). In particular, hAMC-CM reduced H9c2 apoptotic nuclear fragmentation compared with both CTRL-M (−56% $p <$ .001) and fib-CM (−49%; $p <$ .001) and prevented caspase-3 cleavage (Fig. 2B−D). The cytoprotective effects paralleled the concomitant inhibition of both the stress-activated protein kinase/Jun amino-terminal kinase (SAPK/JNK) and p38 mitogen-activated protein kinase (p38 MAPK) proapoptotic pathways and the activation of the extracellular signal-regulated kinase 1/2 mitogen-activated protein kinase (ERK1/2 MAPK); the Akt pathway was not involved (Fig. 2E). Moreover, hAMC-CM led to the concomitant upregulation of the anti-apoptotic genes B-cell lymphoma 2 and signal transducer and activator of transcription 3 and the downregulation of proapoptotic factors Bcl-2 antagonist/killer 1, tumor necrosis factor-α, and Fas ligand (FasL) (Fig. 2E).

We then collected data strongly suggesting that hAMCs positively affect angiogenesis. hAMC-CM remarkably promoted EPC migration in a dose-dependent manner. The number of migrating EPCs fed with hAMC-CM at 1× concentration was significantly increased compared with both CTRL-M (+2.6-fold; $p <$ .01) and fib-CM even when concentrated 50× (+50%; $p <$ .01) (Fig. 3A).

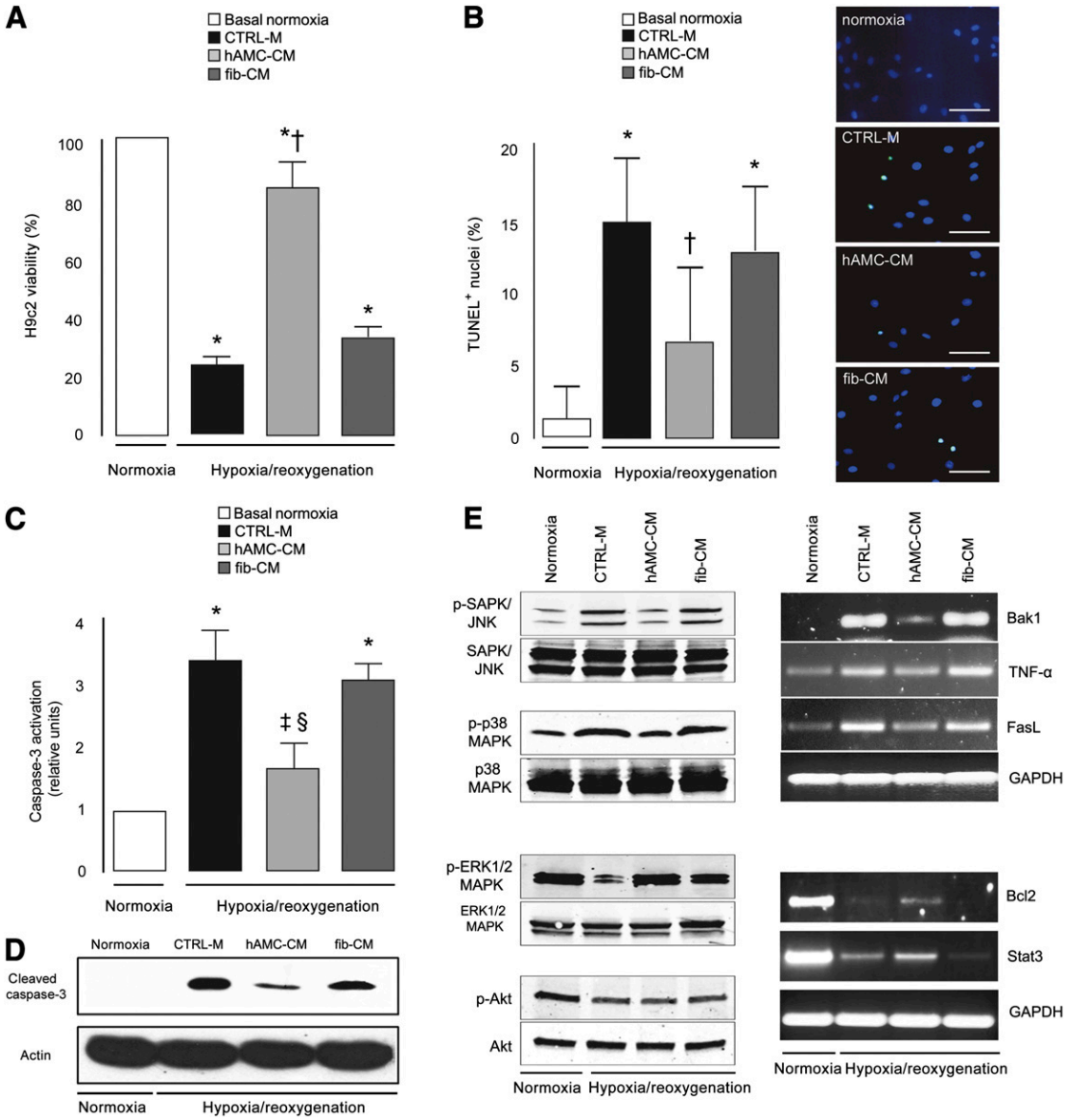

Figure 2. Cytoprotective effect of hAMC-CM in vitro. **(A):** MTS viability assay. **(B):** Quantitative analysis and representative images of the TUNEL assay. Nuclei are shown in blue, and TUNEL$^+$ in green. **(C):** Colorimetric assay of caspase-3 activity. **(D):** Immunoblotting for cleaved caspase-3 (17 kDa). **(E):** Representative images of Western blot (left) and reverse transcription-polymerase chain reaction (right) analysis. *, $p < .001$ versus basal normoxia; †, $p < .001$ versus CTRL-M and fib-CM; ‡, $p < .001$ versus CTRL-M; §, $p < .01$ versus fib-CM. All data expressed as the mean ± SD. Data are representative of three independent experiments. Abbreviations: Bak1, Bcl-2 antagonist/killer 1; Bcl-2, B-cell lymphoma 2; CTRL-M, control medium; ERK1/2 MAPK, extracellular signal-regulated kinase 1/2 mitogen-activated protein kinase; FasL, Fas ligand; fib-CM, human dermal fibroblast conditioned medium; GAPDH, glyceraldehyde 6-phosphate dehydrogenase; hAMC-CM, conditioned medium obtained from human amniotic membrane-derived mesenchymal stromal cells; p, phosphorylated; p38 MAPK = p38 mitogen-activated protein kinase; SAPK/JNK, stress-activated protein kinase/Jun amino-terminal kinase; Stat3, signal transducer and activator of transcription 3; TNF-α, tumor necrosis factor-α; TUNEL, terminal deoxynucleotidyl transferase dUTP nick-end labeling.

The chemoattractive effect of hAMC-CM at 1× was comparable to that exerted by the potent chemoattractant SDF-1α, and, at the 50× concentration, the migration response to hAMC-CM was even higher than in the presence of SDF-1α (+58%; $p < .01$) (Fig. 3A). In addition, the Matrigel assay showed a marked increase in capillary density when EPCs were fed with hAMC-CM compared with CTRL-M (+3.18-fold; $p < .001$) or fib-CM (+16-fold; $p < .001$) (Fig. 3B). Dose-response experiments demonstrated that EPC tube formation was enhanced in the presence of hAMC-CM 20× compared with the lower concentrations, 1× (+32%; $p < .001$) and 10× (+21%; $p < .001$) (Fig. 3C). With fib-CM, we also observed a dose-dependent effect, but the number of branches per field was significantly lower compared with hAMC-CM at each concentration tested (Fig. 3C). Time-course experiments showed that, in the presence of hAMC-CM, capillary-like structures were visible as early as 5 hours and were still present at 24, 48, and 72 hours. In contrast, very few capillaries were observed at the same time points when EPCs were grown in fib-CM (Fig. 3D).

To examine the in vivo relevance of our in vitro findings, we studied the effects of intramyocardial injection of concentrated

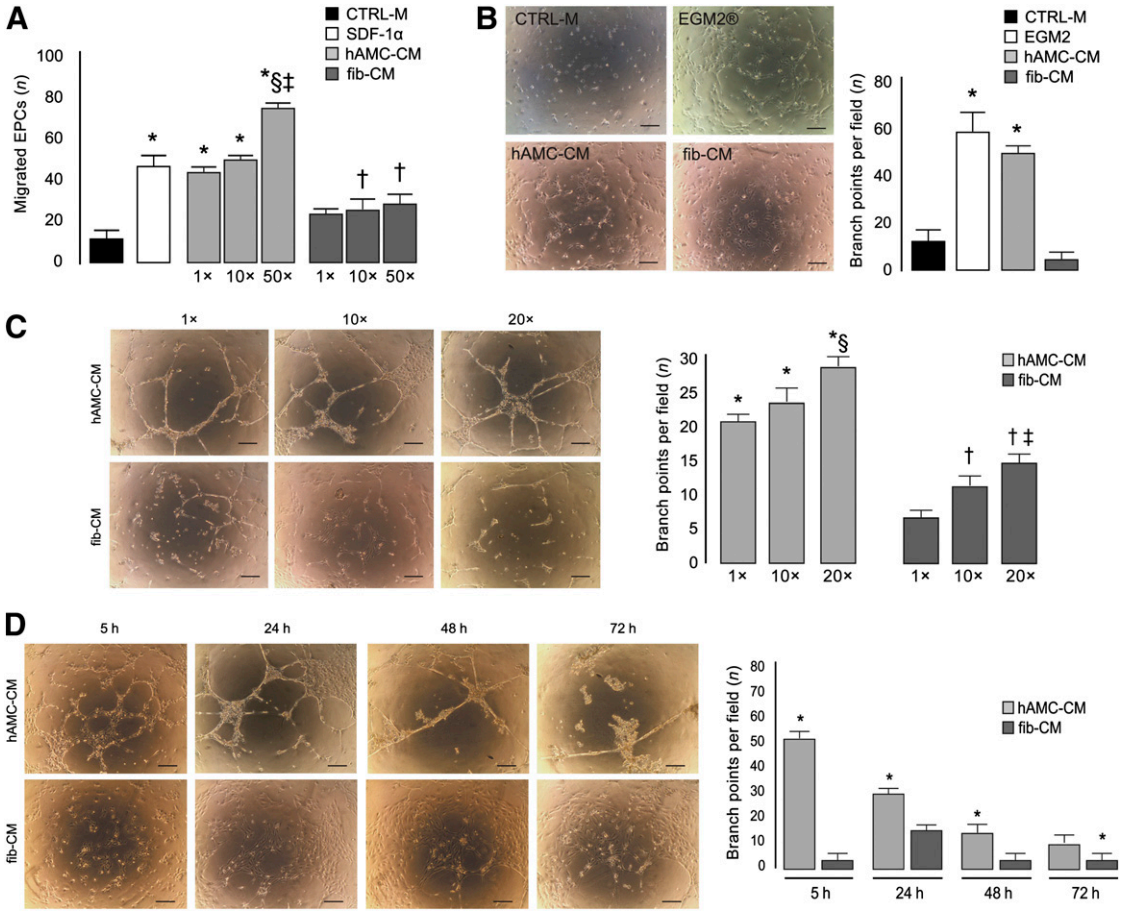

Figure 3. hAMC-CM promotes angiogenesis in vitro. **(A):** Boyden chamber migration assay. $*$, $p < .01$ versus CTRL-M and fib-CM 1×, 10×, and 50×; †, $p < .001$ versus CTRL-M; §, $p < .01$ versus SDF-1α; ‡, $p < .01$ versus hAMC-CM 1× and 10×. **(B):** Representative images of EPCs cultured in Matrigel for 5 hours in the presence of CTRL-M, EGM2 (growth medium), hAMC-CM, or fib-CM and quantification of the number of branches per field. Scale bar = 200 μm. $*$, $p < .001$ versus CTRL-M and fib-CM. **(C):** Representative images of EPCs cultured in Matrigel for 24 hours in the presence of hAMC-CM or fib-CM at 1×, 10×, or 20×. Bars summarize the quantitative analysis. Scale bar = 200 μm. $*$, $p < .001$ versus fib-CM 1×, 10×, and 20×; §, $p < .001$ versus hAMC-CM 1× and 10×; †, $p < .05$ versus fib-CM 1×; ‡, $p < .05$ versus fib-CM 10×. **(D):** Representative images of EPCs cultured in Matrigel in the presence of hAMC-CM 20× or fib-CM 20× for 5, 24, 48, and 72 hours; bars represent the quantitative analysis. Scale bar = 200 μm. $*$, $p < .001$ versus fib-CM. All data are expressed as the mean ± SD. Data are representative of three independent experiments. Abbreviations: CTRL-M, control medium; EGM2, endothelial growth medium 2; EPCs, endothelial progenitor cells; fib-CM, human dermal fibroblast conditioned medium; hAMC-CM, conditioned medium obtained from human amniotic membrane-derived mesenchymal stromal cells; SDF-1α, stromal cell derived factor-1α.

CM using a well-established model of ischemia/reperfusion (I/R) injury in rats. The data on IS support our in vitro cytoprotective results. The infarct zone in the saline-treated group was 46% ± 7% of the AAR. Intramyocardial injection of concentrated hAMC-CM limited IS by 28.5% ($p < .01$) and 28.3% ($p < .01$) compared with saline and fib-CM, respectively (Fig. 4A). In the hearts treated with hAMC-CM, the number of TUNEL$^+$ CMC nuclei at the infarct border zone was reduced compared with both saline (−43.4%; $p < .001$) and fib-CM (−39.4%; $p < .001$) (Fig. 4B), indicating a remarkable anti-apoptotic effect.

The limitation in IS obtained with hAMC-CM resulted in better ventricular remodeling, as documented by morphometric analysis performed at 1 month. Measurements of the LV wall thickness demonstrated that administration of hAMC-CM prevented the thinning of the anterior wall compared with both saline (+27%; $p < .01$) and fib-CM (+30%; $p < .01$). Moreover, the scar area in the hAMC-CM-treated hearts was 42.9% ($p < .01$) and 52.2% ($p < .001$) smaller than those treated saline and fib-CM, respectively (Fig. 4C).

We then quantified the capillary density to examine the possible contribution of neoangiogenesis in the myocardial repair process. Isolectin immunostaining showed that 30 days after hAMC-CM injection, the number of capillaries at the infarct border zone was 100% ($p < .001$) and 36% ($p < .05$) higher compared with saline and fib-CM, respectively (Fig. 5). These data parallel our in vitro results and confirm that hAMC-CM is proangiogenic.

Next, we searched for putative active mediators of cardioprotection and angiogenesis using a combined genome-wide and cytokine array approach. A comparison of the gene expression profiles (Fig. 6A) revealed that 1,682 genes were expressed at significantly different levels by hAMC and fibroblasts. Of those genes, 647 were significantly upregulated in hAMC (supplemental online Table 2) and 131 of these by more than twofold (supplemental online Table 3). Gene Ontology (GO) functional annotation analysis was performed on this latter group of 131 genes. Bar graphs reporting the percentage of annotated genes in each group are illustrated in supplemental online Figures 1 and 2 (GO

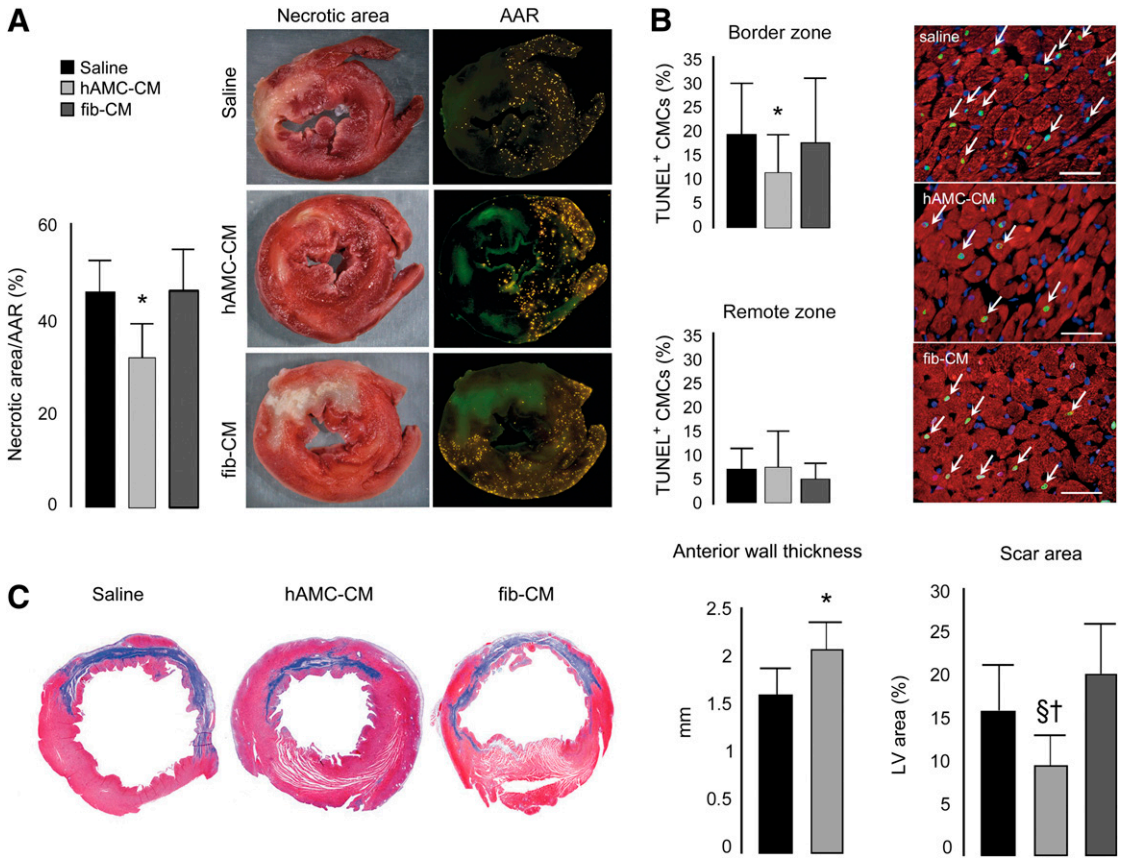

Figure 4. Effects of hAMC-CM on cardioprotection and ventricular remodeling in vivo. **(A):** Infarct size assessment ($n = 10$ animals per group). $*$, $p < .01$ versus saline and fib-CM. **(B):** TUNEL assay: α-sarcomeric actin in red, nuclei in blue, and TUNEL$^+$ in green (white arrows). Scale bar = 50 μm. $*$, $p < .001$ versus saline and fib-CM. Apoptotic index was quantified with 10,000 cardiomyocytes. **(C):** Quantitative analysis of LV morphometric parameters ($n = 8$ animals per group) were calculated as described in the supplemental online data. $*$, $p < .01$ versus saline and versus fib-CM; †, $p < .001$ versus fib-CM; §, $p < .01$ versus saline. Abbreviations: AAR, area at risk; CMCs, cardiomyocytes; fib-CM, human dermal fibroblast conditioned medium; hAMC-CM, conditioned medium obtained from human amniotic membrane-derived mesenchymal stromal cells; LV, left ventricular; TUNEL, terminal deoxynucleotidyl transferase dUTP nick-end labeling.

for cellular component and GO for biological process, respectively). The lists of genes belonging to each enriched group are listed in supplemental online Tables 4 and 5. Significant GO terms identified by cellular component analysis were mostly related to the extracellular region (GO:0005576), extracellular matrix (GO:0031012), and collagen (GO:0005581), suggesting that the expression of these secreted factors is highly enriched in hAMCs. Furthermore, when a search for a correlation with the biological function of the upregulated genes was performed, GO terms involving cell adhesion (GO:0007155), biological adhesion (GO:0022610), response to wounding (GO:0009611), extracellular matrix organization (GO:0030198), blood vessel development (GO:0001568), vasculature development (GO:0001944), collagen fibril organization (GO:0030199), regulation of cell adhesion (GO:0030155), response to oxidative stress (GO:0006979), and response to reactive oxygen species (GO:0000302) were the most significantly enriched terms.

A thorough individual study of the 32 genes annotated with the GO term extracellular region (GO:0005576), listed in supplemental online Table 1, led to the identification of midkine (MDK; +2.6-fold vs. fibroblasts) and secreted protein, acidic, cysteine-rich (SPARC; +2.4-fold vs. fibroblasts), as interesting putative paracrine cardioprotective mediators [15, 16]. Quantitative polymerase chain reaction confirmed the data obtained with the array, documenting that, compared with fibroblasts, both MDK (+8-fold; $p < .001$) and SPARC (+5.8-fold; $p < .001$) were increased in hAMCs (Fig. 6B). Western blot analysis of these proteins in CM samples confirmed that both MDK and SPARC were highly secreted in hAMC-CM compared with fib-CM (Fig. 6C). We also identified several genes encoding for putative secreted proteins with unknown functions that might potentially exert beneficial effects on the ischemic myocardium (data not shown).

Finally, through cytokine antibody array, we demonstrated that hAMCs produce high amounts of several proangiogenic factors that likely mediate the effects observed on EPCs and capillary formation (Fig. 7). hAMCs secreted all 20 cytokines assayed. Among these, angiogenin, platelet-derived growth factor-BB (PDGF-BB), basic fibroblast growth factor (bFGF), insulin-like growth factor 1 (IGF-1), thrombopoietin, vascular endothelial growth factor (VEGF), and VEGF-D were highly enriched in hAMC-CM compared with fib-CM ($p < .05$).

Discussion

Acute myocardial infarction (AMI) remains the leading cause of mortality and morbidity worldwide [17]. Timely pharmacological

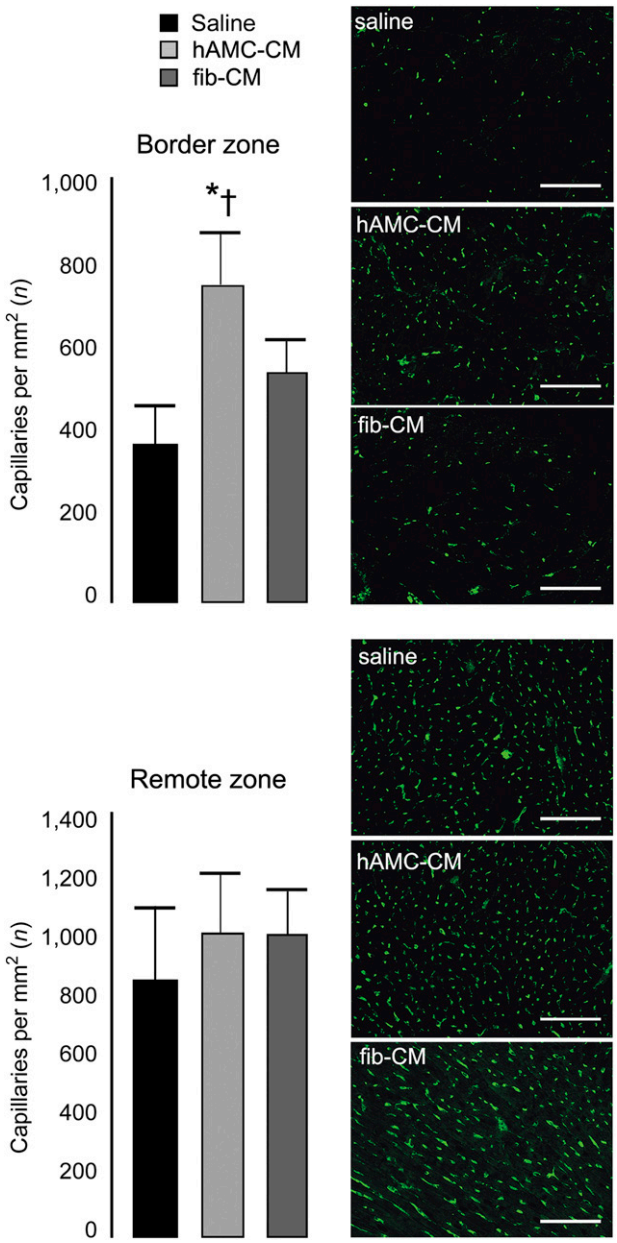

Figure 5. Proangiogenic effects of hAMC-CM in vivo. Capillary density was assessed by isolectin B4 immunostaining (green) at both the border and the remote zone ($n = 5$ animals per group). Scale bar = 100 μm. *, $p < .001$ versus saline; †, $p < .05$ versus fib-CM. All data are expressed as the mean ± SD. Abbreviations: fib-CM, human dermal fibroblast conditioned medium; hAMC-CM, conditioned medium obtained from human amniotic membrane-derived mesenchymal stromal cells.

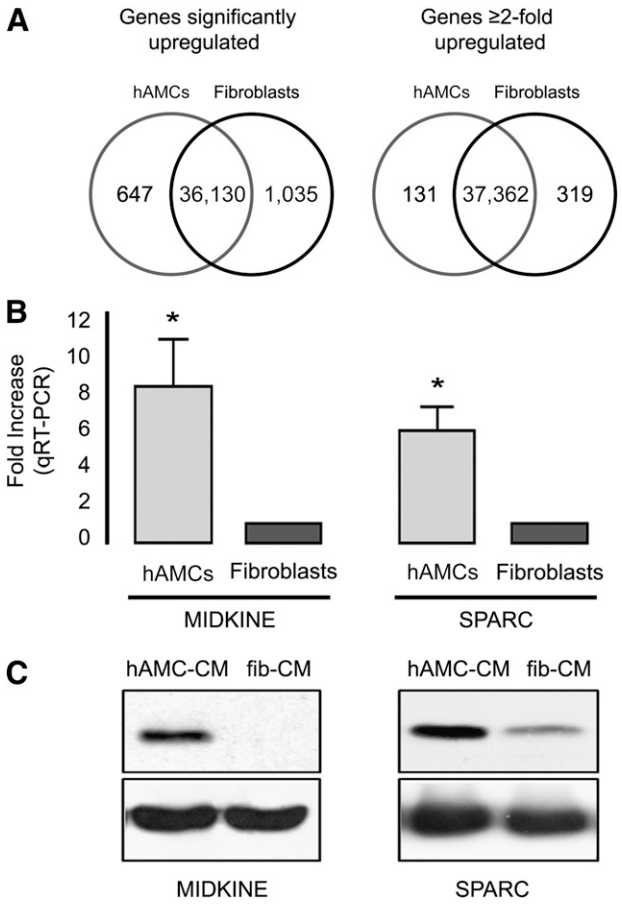

Figure 6. Identification of paracrine active mediators. **(A):** Venn diagrams representing the number of detected genes significantly upregulated (left) and upregulated more than twofold (right) in hAMCs and fibroblasts. **(B)** qRT-PCR validation analysis of MDK and SPARC expression in hAMC and fibroblasts. The bar graph represents the fold increase expression value of hAMC-CM compared with fibroblasts. *, $p < .001$. Data are expressed as the mean ± SD. Data are representative of three independent experiments (two replicates each). **(C):** Representative Western blot analysis of MDK (14.6 kDa, left) and SPARC (35 kDa, right) in hAMC-CM and fib-CM. Data are representative of three independent experiments. Abbreviations: fib-CM, human dermal fibroblast conditioned medium; hAMCs, human amniotic membrane-derived mesenchymal stromal cells; hAMC-CM, conditioned medium obtained from hAMCs; qRT-PCR, quantitative reverse transcription-polymerase chain reaction; SPARC, secreted protein, acidic, cysteine-rich.

or mechanical reperfusion of an occluded coronary artery represents the most effective therapy to spare the cardiac tissue from ischemic damage [18]. Many adjuvant medications, such as powerful antiplatelet and anticoagulant drugs, have been shown to further ameliorate the outcome of subjects experiencing AMI. However, even after the best medical treatment, in many patients, the IS is still significantly extended, and negative LV remodeling ensues [17].

With the present study, we provide evidence that hAMCs produce and release factors able to promote cardiac repair. Two important aspects of stem cell action were studied both in vitro and in vivo: cardioprotection and neoangiogenesis.

We demonstrated that hAMC-CM strongly protects cardiac-like cells from H/R injury in vitro. The main mechanism revealed was inhibition of cell apoptosis, shown by the reduction in nuclear fragmentation and caspase activation. In the presence of hAMC-CM, the prosurvival ERK1/2 MAPK pathway is clearly activated and proapoptotic pathways such as SAPK/JNK and p38 MAPK are inhibited. Likewise, hAMC-CM activates prosurvival genes and prevents the activation of proapoptotic genes in cardiac cells. The cardioprotective effect exerted by hAMC-CM was also meaningful in vivo, as verified by the significant limitation in IS and cardiac apoptosis in rat hearts. The 28.5% limitation in IS observed after hAMC-CM treatment was comparable to that observed in infarcted pig hearts treated with ischemic postconditioning,

A

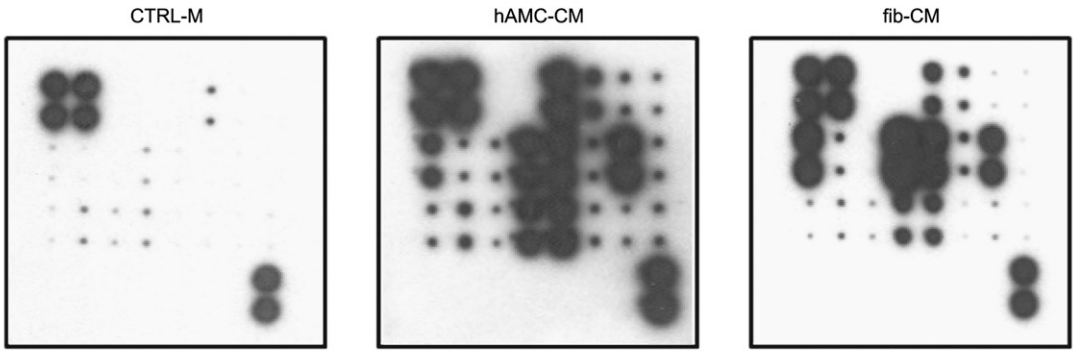

B

POS	POS	NEG	NEG	Angiogenin	EGF	ENA-78	bFGF
POS	POS	NEG	NEG	Angiogenin	EGF	ENA-78	bFGF
GRO	IFN-γ	IGF-I	IL-6	IL-8	LEPTIN	MCP-1	PDGF-BB
GRO	IFN-γ	IGF-I	IL-6	IL-8	LEPTIN	MCP-1	PDGF-BB
PlGF	RANTES	TGF-β1	TIMP-1	TIMP-2	Thrombopoietin	VEGF	VEGF-D
PlGF	RANTES	TGF-β1	TIMP-1	TIMP-2	Thrombopoietin	VEGF	VEGF-D
Blank	Blank	Blank	Blank	Blank	Blank	NEG	POS
Blank	Blank	Blank	Blank	Blank	Blank	NEG	POS

Note: GRO detects CXCL1, CXCL2, CXCL3; TGF-β1 detects only active forms; VEGF detects VEGF-165 and VEGF-121

C

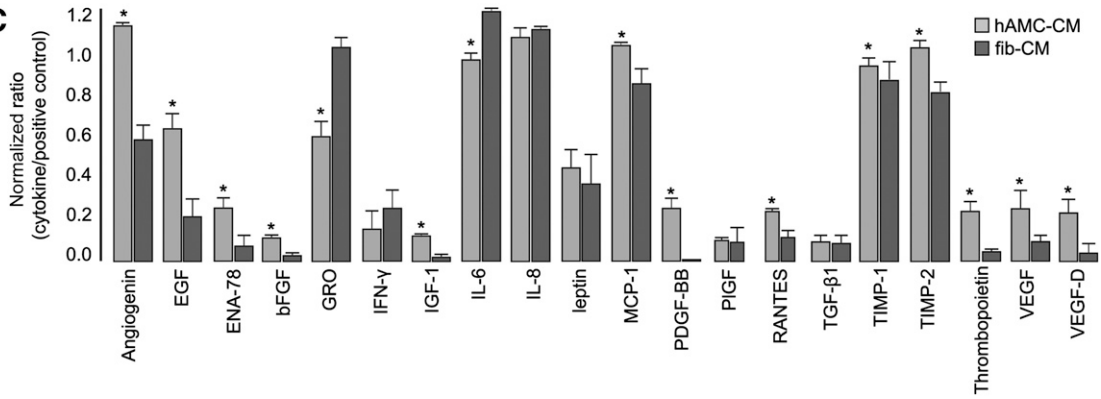

Figure 7. Proangiogenic factors present in the hAMC-CM. **(A):** Representative images of human cytokine antibody array membranes (RayBio Human Angiogenesis Antibody array I, RayBiotech, Norcross, GA, http://www.raybiotech.com) of CTRL-M, hAMC-CM, and fib-CM. **(B):** Layout of the membrane for the human cytokine antibody array. Positive controls are located in the upper left corner (four spots) and lower right corner (two spots) of each membrane. **(C):** Quantitative analysis confirmed that several proangiogenic cytokines are significantly more abundant in hAMC-CM than in fib-CM. $*$, $p < .05$ versus fib-CM. All data are expressed as the mean $\pm$ SD. Data are representative of two independent experiments. Abbreviations: bFGF, basic fibroblast growth factor; CTRL-M, control medium; EGF, endothelial growth factor; ENA-78 or CXCL5, C-X-C motif chemokine 5; fib-CM, human dermal fibroblast conditioned medium; GRO, growth-regulated oncogene; hAMC-CM, human amniotic membrane-derived mesenchymal stromal cells conditioned medium; IFN-γ, interferon-γ; IGF-1, insulin-like growth factor 1; IL, interleukin; MCP-1, monocyte chemoattractant protein-1; Neg, negative; PlGF, placental growth factor; PDGF, platelet-derived growth factor; Pos, positive; RANTES, regulated on activation, normal T cell expressed and secreted; TGF-β1, transforming growth factor-β1; TIMP, tissue inhibitor of metalloproteinase; VEGF, vascular endothelial growth factor.

currently considered the most attractive approach to achieve cardioprotection [19, 20]. The smaller IS prevented wall thinning and LV enlargement, as documented by morphometric analysis performed at 1 month.

The effect of hAMC-CM was not limited to cardioprotection. As demonstrated by in vitro assays and confirmed in vivo, the soluble factors secreted by hAMC strongly promoted neovascularization. In vitro, the effects triggered by hAMC-CM equaled those obtained with SDF-1α, and in vivo, hAMC-CM significantly increased the number of capillaries at the infarct border zone compared with saline. This result is comparable to, if not greater than, that obtained with other potent proangiogenic therapies, including injection of endothelial early outgrowth progenitor cells isolated from healthy patients [21], gene therapy with VEGF2 [22], and administration of human recombinant bFGF [23], to name a few. These results can be partially explained because several proangiogenic factors are abundantly secreted by hAMCs, as shown by our cytokine profiling, including VEGF, bFGF, IGF-1, thrombopoietin, PDGF-BB, angiogenin, and VEGF-D.

Although this was not the main goal of the present study, we attempted to shed light on the putative soluble mediators of the observed cardioprotective effects. We performed whole-genome expression profiling on hAMCs, which currently represents a more comprehensive and technically less demanding method than

proteomics. We identified genes overexpressed in hAMCs compared with fibroblasts. We then focused our genomic analysis on the genes encoding the secreted proteins, and, by computational analysis, we identified 32 genes encoding known secreted factors. Although this strategy does not provide direct evidence that these particular factors are responsible for the observed cardioprotective effects, it does show that hAMCs overexpress several candidate soluble molecules. Furthermore, we evaluated the function of each individual secreted factor by surveying the published data. MDK and SPARC emerged as the two most interesting candidates of putative hAMC-secreted proteins exerting prosurvival effects on the myocardium. MDK has been shown to reduce apoptosis via ERK phosphorylation and by Bcl-2 activation in mice subjected to I/R [24]. In addition, it has been shown that exogenous MDK attenuates LV remodeling and improves long-term survival after a myocardial infarct by enhancing angiogenesis and reducing apoptosis via the Akt/PI3-kinase pathway [15, 25, 26]. SPARC exerts a key role in collagen assembly in the extracellular matrix [16]. The absence of SPARC results in a significant increase in myocardial rupture and ventricular dysfunction after myocardial infarct [27]. Consistently, overexpression of SPARC by adenoviral delivery in wild-type mice 2 days before myocardial infarction resulted in improved cardiac function and a reduction in dilation without significant effects on IS [27].

As expected, most of the genes upregulated in the hAMCs coded either for proteins with unknown function or for secreted proteins without a previously described cardioprotective function. Thus, we cannot exclude the fascinating possibility that among these genes, some might code for powerful novel therapeutic molecules that could contribute to the beneficial effects we have described. The identification of these putative factors will require many additional studies over the next few years. For example, the next challenging goal will be to flank the reported genomic approach with a proteomic and functional approach aimed at dissecting the complete nature and scope of the factors involved in the therapeutic effects conferred by the CM obtained from hAMCs.

It has also been proposed that the beneficial cardioprotective effects observed after MSC therapy might be mediated by exosomes [28]. Exosomes are small vesicles (between 30 and 100 nm in diameter) of endocytotic origin, limited by a lipid bilayer containing cytosol, and secreted by most cells. In addition to cardioprotection, it has been suggested that exosomes can favor angiogenesis by modulating the soluble factor production involved in endothelial and progenitor cell differentiation, proliferation, migration, and adhesion [29]. The exact mechanism of action of exosomes is still partially unknown, although it is likely that, in the end, the real mediators might be the proteins and/or the microRNA contained inside the exosomes and released by the microparticles on entry to the target cells [30]. The role of exosomes in hAMC paracrine action needs to be elucidated.

Conclusion

The demonstration that stem cells secrete therapeutic factors provides a potential breakthrough. Characterization of those paracrine mediators could lead to the replacement of stem cell-based therapy with a soluble factor-based therapy in which a single or a mixture of molecules would be administered to patients [31]. A shortcut approach might consist of the administration of the entire stem cell secretome (i.e., conditioned medium). This strategy, compared with cell therapy, would be technically simpler to translate to the bedside.

Despite these potential advantages, this approach has not been properly investigated using human cells. The only exception is represented by MSCs derived from embryonic stem cells, a source that is ethically unacceptable for many patients. Several strategies have been pursued to modulate and magnify the production of paracrine factors [32–34]. However, every additional manipulation step in the production of a therapeutic cell-derived product represents a hurdle to its clinical translation for both safety and cost reasons. We have demonstrated that CM of fetal stromal cells, derived from an ethically acceptable source, such as the placenta, can repair infarcted hearts without the need for any manipulation. Nevertheless, transplantation of stem cells still represents a reasonable strategy. Our results, contributing to those showing their direct cardiac regeneration potential and their immunoprivileged phenotype, support the concept that hAMCs are excellent candidates for cardiac cell therapy.

Acknowledgments

We acknowledge Laurene Kelly for expert editorial support. This work was supported by the Ministero Italiano della Sanità (Grants GR-2008-1142781, GR-2010-2320533), the Fondazione Cariplo (Grant 2007-5984), and the Ministero Italiano degli Affari Esteri (Grant ZA11GR2).

Author Contributions

P.D., G.M., and M.C.C.: conception and design, collection and/or assembly of data, data analysis and interpretation, manuscript writing; E.C., L.C. F.C., F.P., M.M., L.K., and R.d.B.: collection and/or assembly of data; G.V. and V.R.: collection and/or assembly of data, data analysis and interpretation; A.S. and M.R.: provision of study material or patients; M.G.: conception and design, financial support, collection and/or assembly of data, data analysis and interpretation, manuscript writing, final approval of manuscript.

Disclosure of Potential Conflicts of Interest

The authors indicated no potential conflicts of interest.

References

1 Anversa P, Kajstura J, Rota M et al. Regenerating new heart with stem cells. J Clin Invest 2013;123:62–70.

2 Gnecchi M, Danieli P, Cervio E. Mesenchymal stem cell therapy for heart disease. Vascul Pharmacol 2012;57:48–55.

3 Noiseux N, Gnecchi M, Lopez-Ilasaca M et al. Mesenchymal stem cells overexpressing Akt dramatically repair infarcted myocardium and improve cardiac function despite infrequent cellular fusion or differentiation. Mol Ther 2006;14:840–850.

4 Gnecchi M, Zhang Z, Ni A et al. Paracrine mechanisms in adult stem cell signaling and therapy. Circ Res 2008;103:1204–1219.

5 Gnecchi M, He H, Liang OD et al. Paracrine action accounts for marked protection of ischemic heart by Akt-modified mesenchymal stem cells. Nat Med 2005;11:367–368.

6 Gnecchi M, He H, Noiseux N et al. Evidence supporting paracrine hypothesis for Akt-modified mesenchymal stem cell-mediated cardiac protection and functional improvement. FASEB J 2006;20:661–669.

7 Kinnaird T, Stabile E, Burnett MS et al. Marrow-derived stromal cells express genes encoding a broad spectrum of arteriogenic

cytokines and promote in vitro and in vivo arteriogenesis through paracrine mechanisms. Circ Res 2004;94:678–685.

8 Gnecchi M, He H, Melo LG et al. Early beneficial effects of bone marrow-derived mesenchymal stem cells overexpressing Akt on cardiac metabolism after myocardial infarction. STEM CELLS 2009;27:971–979.

9 Hatzistergos KE, Quevedo H, Oskouei BN et al. Bone marrow mesenchymal stem cells stimulate cardiac stem cell proliferation and differentiation. Circ Res 2010;107:913–922.

10 In 't Anker PS, Scherjon SA, Kleijburg-van der Keur C et al. Isolation of mesenchymal stem cells of fetal or maternal origin from human placenta. STEM CELLS 2004;22:1338–1345.

11 Portmann-Lanz CB, Schoeberlein A, Huber A et al. Placental mesenchymal stem cells as potential autologous graft for pre- and perinatal neuroregeneration. Am J Obstet Gynecol 2006;194:664–673.

12 Sakuragawa N, Kakinuma K, Kikuchi A et al. Human amnion mesenchyme cells express phenotypes of neuroglial progenitor cells. J Neurosci Res 2004;78:208–214.

13 Tsuji H, Miyoshi S, Ikegami Y et al. Xenografted human amniotic membrane-derived mesenchymal stem cells are immunologically tolerated and transdifferentiated into cardiomyocytes. Circ Res 2010;106:1613–1623.

14 Edgar R, Domrachev M, Lash AE. Gene Expression Omnibus: NCBI gene expression and hybridization array data repository. Nucleic Acids Res 2002;30:207–210.

15 Sumida A, Horiba M, Ishiguro H et al. Midkine gene transfer after myocardial infarction in rats prevents remodelling and ameliorates cardiac dysfunction. Cardiovasc Res 2010;86:113–121.

16 McCurdy S, Baicu CF, Heymans S et al. Cardiac extracellular matrix remodeling: Fibrillar collagens and secreted protein acidic and rich in cysteine (SPARC). J Mol Cell Cardiol 2010;48:544–549.

17 Go AS, Mozaffarian D, Roger VL et al. Heart disease and stroke statistics—2013 Update: A report from the American Heart Association. Circulation 2013;127:e6–e245.

18 Task Force on the management of ST-segment elevation acute myocardial infarction of the European Society of Cardiology (ESC), Steg PG, James SK et al. ESC guidelines for the management of acute myocardial infarction in patients presenting with ST-segment elevation. Eur Heart J 2012;33:2569–2619.

19 Heusch G, Musiolik J, Gedik N et al. Mitochondrial STAT3 activation and cardioprotection by ischemic postconditioning in pigs with regional myocardial ischemia/reperfusion. Circ Res 2011;109:1302–1308.

20 Heusch G. Cardioprotection: Chances and challenges of its translation to the clinic. Lancet 2013;381:166–175.

21 Jakob P, Doerries C, Briand S et al. Loss of angiomiR-126 and 130a in angiogenic early outgrowth cells from patients with chronic heart failure: Role for impaired in vivo neovascularization and cardiac repair capacity. Circulation 2012;126:2962–2975.

22 Kawamoto A, Murayama T, Kusano K et al. Synergistic effect of bone marrow mobilization and vascular endothelial growth factor-2 gene therapy in myocardial ischemia. Circulation 2004;110:1398–1405.

23 Yanagisawa-Miwa A, Uchida Y, Nakamura F et al. Salvage of infarcted myocardium by angiogenic action of basic fibroblast growth factor. Science 1992;257:1401–1403.

24 Horiba M, Kadomatsu K, Yasui K et al. Midkine plays a protective role against cardiac ischemia/reperfusion injury through a reduction of apoptotic reaction. Circulation 2006;114:1713–1720.

25 Takenaka H, Horiba M, Ishiguro H et al. Midkine prevents ventricular remodeling and improves long-term survival after myocardial infarction. Am J Physiol Heart Circ Physiol 2009;296:H462–H469.

26 Kadomatsu K, Bencsik P, Görbe A et al. Therapeutic potential of midkine in cardiovascular disease. Br J Pharmacol 2014;171:936–944.

27 Schellings MW, Vanhoutte D, Swinnen M et al. Absence of SPARC results in increased cardiac rupture and dysfunction after acute myocardial infarction. J Exp Med 2009;206:113–123.

28 Lai RC, Arslan F, Lee MM et al. Exosome secreted by MSC reduces myocardial ischemia/reperfusion injury. Stem Cell Res (Amst) 2010;4:214–222.

29 Martinez MC, Andriantsitohaina R. Microparticles in angiogenesis: Therapeutic potential. Circ Res 2011;109:110–119.

30 Ailawadi S, Wang X, Gu H et al. Pathologic function and therapeutic potential of exosomes in cardiovascular disease. Biochim Biophys Acta 2015;1852:1–11.

31 Timmers L, Lim SK, Hoefer IE et al. Human mesenchymal stem cell-conditioned medium improves cardiac function following myocardial infarction. Stem Cell Res (Amst) 2011;6:206–214.

32 Mangi AA, Noiseux N, Kong D et al. Mesenchymal stem cells modified with Akt prevent remodeling and restore performance of infarcted hearts. Nat Med 2003;9:1195–1201.

33 Matsumoto R, Omura T, Yoshiyama M et al. Vascular endothelial growth factor-expressing mesenchymal stem cell transplantation for the treatment of acute myocardial infarction. Arterioscler Thromb Vasc Biol 2005;25:1168–1173.

34 Tang YL, Tang Y, Zhang YC et al. Improved graft mesenchymal stem cell survival in ischemic heart with a hypoxia-regulated heme oxygenase-1 vector. J Am Coll Cardiol 2005;46:1339–1350.

See www.StemCellsTM.com for supporting information available online.